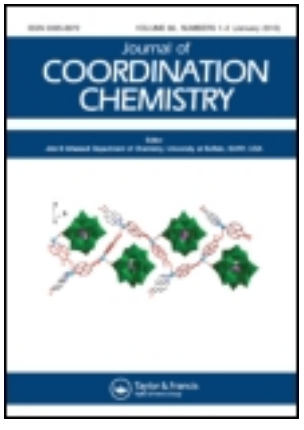

Journal of Coordination Chemistry
Publication details, including instructions for authors and subscription information:
http://www.tandfonline.com/loi/gcoo20

DNA interaction studies of d^9 and d^{10} metal complexes having Schiff base and polypyridyl ligands

Krishnan Pothiraj [a], Thanasekaran Baskaran [a] & Natarajan Raman [a]

[a] Research Department of Chemistry, VHNSN College, Virudhunagar-626001, India

Accepted author version posted online: 03 May 2012.Published online: 16 May 2012.

To cite this article: Krishnan Pothiraj, Thanasekaran Baskaran & Natarajan Raman (2012) DNA interaction studies of d^9 and d^{10} metal complexes having Schiff base and polypyridyl ligands, Journal of Coordination Chemistry, 65:12, 2110-2126, DOI: 10.1080/00958972.2012.690037

To link to this article: http://dx.doi.org/10.1080/00958972.2012.690037

Journal of Coordination Chemistry
Vol. 65, No. 12, 20 June 2012, 2110–2126

DNA interaction studies of d^9 and d^{10} metal complexes having Schiff base and polypyridyl ligands

KRISHNAN POTHIRAJ, THANASEKARAN BASKARAN and NATARAJAN RAMAN*

Research Department of Chemistry, VHNSN College, Virudhunagar-626001, India

(*Received 12 December 2011; in final form 20 March 2012*)

Four mononuclear complexes of Cu(II) and Zn(II) having a Schiff-base ligand and 1,10-phenanthroline/2,2′-bipyridine have been synthesized and characterized. From electronic spectral and magnetic susceptibility data, octahedral geometry has been proposed for the complexes. DNA-binding behaviors of these complexes are studied by absorption titration, electrochemical, and viscosity methods. The results indicate that the complexes bind to calf thymus DNA in an intercalative mode. The gel electrophoresis results reveal that **1** cleaves pBR322 DNA effectively. The ligand and its complexes have been screened for their antimicrobial activities against a few microorganisms. The data exhibit that they are better antimicrobial agents than the ligand.

Keywords: Schiff base; DNA-Binding; DNA Cleavage; Antimicrobial activity

1. Introduction

Transition metal complexes such as ruthenium, rhodium, cobalt, nickel, copper, zinc, and lanthanum with nitrogen containing heterocyclic ligands [1, 2] have shown binding and cleavage activities with DNA [3, 4]. Planar condensed aromatic ligands such as 1,10-phenanthroline, bipyridine, and their derivatives (whose donor properties are similar to purine and pyrimidine bases) in antitumor (DNA-binding) agents have drawn attention to their promising properties [5, 6].

These metal complexes are also useful for design and development of synthetic restriction enzymes, new drugs, DNA foot printing agents etc., because of their potential to bind DNA and to cleave the duplex [7–10]. The ligands and metal are of paramount importance in interaction of complexes with DNA, understanding of which would help in design of new drugs and development of new selective, efficient DNA recognition, and cleaving agents [11].

Copper(II) complexes play a significant role either as naturally occurring biological systems or as pharmacological agents [12, 13]. Copper plays an important role in hematopoiesis, the central nervous system, and bone tissue [14, 15]. Moreover, due to the ability of copper(II) complexes to cleave DNA, many find possible medical uses

*Corresponding author. Email: drn_raman@yahoo.co.in

ISSN 0095-8972 print/ISSN 1029-0389 online © 2012 Taylor & Francis
http://dx.doi.org/10.1080/00958972.2012.690037

in the treatment of diseases including cancer [16]. Among the various copper complexes so far investigated, those containing phenanthroline and its derivatives have attracted attention for their various biological activities such as antimycobacterial and antimicrobial activities [17, 18]. We reported herein the synthesis and characterization of Schiff base with polypyridyl copper(II) and zinc(II) complexes. The DNA-binding properties of these compounds have been studied by electronic absorption spectra, electrochemical, and viscosity measurements. The plasmid DNA cleavage of the complex is also established. The bioefficacy of these complexes are examined against the growth of the several microorganisms.

2. Experimental

2.1. *Chemicals*

2-Methylacetoacetanilide was obtained from Sigma Aldrich, Bangalore (India); 1,10-phenanthroline monohydrate (phen), 2,2′ bipyridyl (bpy), *o*-aminophenol, $CuCl_2 \cdot 2H_2O$, and $ZnCl_2$ were obtained from Merck. All other chemicals and solvents (AR grade) were purchased from commercial sources and used without purification. Doubly distilled water was used to prepare the buffer solutions. Supercoiled plasmid (SC) pBR322 DNA and Tris-HCl buffer were purchased from Bangalore Genei (India). Calf thymus DNA (ct-DNA), agarose (molecular biology grade), and ethidium bromide (EB) were obtained from Sigma (USA). The spectroscopic titration was carried out in aerated buffer (5 mmol L^{-1} Tris-HCl/50 mmol L^{-1} NaCl, pH 7.2) at room temperature.

2.2. *Synthesis of Schiff base (HL)*

The Schiff base has been synthesized by refluxing hot ethanol solution (25 mL) of *o*-aminophenol (1.08 g, 0.01 mol), and hot ethanol solution (40 mL) of 2-methylacetoacetanilide (1.91 g, 0.01 mol) for 4 h. The precipitate formed after evaporation was filtered, washed with cold ethanol, recrystallized from hot ethanol, and dried in air.

$C_{17}H_{18}N_2O_2$: Yield (%): 79.78, orange red, m.p.: 86°C, M. Wt: 282.34, Anal. Calcd (%): C, 72.32; H, 6.43; N, 9.92. Found (%): C, 72.25; H, 6.38; N, 9.89; ^{1}H NMR (DMSO-d_6, δ/ppm): 2.05 (s, 3H, aliphatic–CH_3), 2.48 (s, 3H, aromatic–CH_3), 3.35 (s, 2H, C–CH_2–C), 6.82–7.90 (m, 8H, aromatic–H), 8.95 (s, 1H, CONH), 10.54 (s, 1H, phenolic–OH); IR (KBr, ν/cm^{-1}): 3375 ν(OH), 3238 ν(NH), 3052 ν(Ar–CH), 2980, 2920, ν(aliphatic–CH), 1670 ν(CONH), 1612 ν(CN), 1546 ν(Ar–CC), 1265 ν(C–O). UV-Vis (λ_{max}/nm) (DMF): 242, 273, 335.

2.3. *Synthesis of metal complexes (1–4)*

To a hot suspension of HL (0.282 g, 0.001 mol) in 15 mL ethanol, solution of copper(II) chloride dihydrate (0.170 g, 0.001 mol) or zinc(II) chloride (0.136 g, 0.001 mol) in 20 mL ethanol was added followed by the addition of 1,10-phenanthroline (0.180 g, 0.001 mol)/ 2,2′-bipyridine (0.156 g, 0.001 mol). The mixture was refluxed with stirring for 2 h and cooled to room temperature. The precipitated complexes were filtered off, washed with

ethanol, and dried in a desiccator over anhydrous calcium chloride under vacuum. The dried complexes were subjected to elemental and spectroscopic analysis.

[Cu(L)(phen)Cl] (**1**): Yield (%): 67.25, dark green, m.p.: 162°C, M. Wt: 559.54, Anal. Calcd for $C_{29}H_{25}N_4O_2CuCl$ (%): Cu, 11.33; C, 62.13; H, 4.49; N, 9.99; Cl, 6.32. Found (%): Cu, 11.29; C, 62.14; H, 4.45; N, 9.97; Cl, 6.30; IR (KBr, ν/cm^{-1}): 3237 ν(NH), 3048 ν(Ar–CH), 2984, 2920, ν(aliphatic–CH), 1658 ν(CONH), 1585 ν(CN), 1549 ν(Ar–CC), 1317 ν(C–O), 559 ν(Cu–O), 426 ν(Cu–N); UV-Vis (λ_{max} nm^{-1}) (DMF): 252, 279, 431, 656; molar conductance (DMF): 30.43 Ohm^{-1} cm^2 mol^{-1}; μ_{eff} (B.M): 1.78.

[Cu(L)(bpy)Cl] (**2**): Yield (%): 68.12, light green, m.p.: 154°C, M. Wt: 535.52, Anal. Calcd for $C_{27}H_{25}N_4O_2CuCl$ (%): Cu, 11.84; C, 60.44; H, 4.69; N, 10.44; Cl, 6.60. Found (%): Cu, 11.82; C, 60.41; H, 4.67; N, 10.42; Cl, 6.57; IR (KBr, ν/cm^{-1}): 3239 ν(NH), 3051 ν(Ar–CH), 2982, 2918, ν(aliphatic–CH), 1657 ν(CONH), 1600 ν(CN), 1548 ν(Ar–CC), 1325 ν(C–O), 555 ν(Cu–O), 423 ν(Cu–N); UV-Vis (λ_{max} nm^{-1}) (DMF): 248, 275, 435, 638; molar conductance (DMF): 28.25 Ohm^{-1} cm^2 mol^{-1}; μ_{eff} (B.M): 1.76.

[Zn(L)(phen)Cl] (**3**): Yield (%): 65.56, yellow, m.p.: 151°C, M. Wt: 561.39, Anal. Calcd for $C_{29}H_{25}N_4O_2ZnCl$ (%): Zn, 11.62; C, 61.93; H, 4.48; N, 9.96; Cl, 6.30. Found (%): Zn, 11.59; C, 61.91; H, 4.44; N, 9.94; Cl, 6.28; ^{1}H NMR (DMSO-d$_6$, δ/ppm): 2.06 (s, 3H, aliphatic–CH_3), 2.49 (s, 3H, aromatic–CH_3), 3.36 (s, 2H, C–CH_2–C), 6.84–8.61 (m, 16H, aromatic–H), 8.98 (s, 1H, CONH). IR (KBr, ν/cm^{-1}): 3238 ν(NH), 3050 ν(Ar–CH), 2981, 2925 ν(aliphatic–CH), 1654 ν(CONH), 1597 ν(CN), 1551 ν(Ar–CC), 1320 ν(C–O), 565 ν(Zn–O), 435 ν(Zn–N); UV-Vis (λ_{max} nm^{-1}) (DMF): 250, 282, 437; molar conductance (DMF): 29.58 Ohm^{-1} cm^2 mol^{-1}; μ_{eff} (B.M): diamagnetic.

[Zn(L)(bpy)Cl] (**4**): Yield (%): 67.74, yellow, m.p.: 145°C, M. Wt: 537.37, Anal. Calcd for $C_{27}H_{25}N_4O_2ZnCl$ (%): Zn, 12.14; C, 60.23; H, 4.68; N, 10.40; Cl, 6.58. Found (%): Zn, 12.12; C, 60.20; H, 4.64; N, 10.38; Cl, 6.56; ^{1}H NMR (DMSO-d$_6$, δ/ppm): 2.05 (s, 3H, aliphatic–CH_3), 2.48 (s, 3H, aromatic–CH_3), 3.36 (s, 2H, C–CH_2–C), 6.83–8.48 (m, 16H, aromatic–H), 8.96 (s, 1H, CONH). IR (KBr, ν/cm^{-1}): 3238 ν(NH), 3050 ν(Ar–CH), 2980, 2923 ν(aliphatic–CH), 1656 ν(CONH), 1588 ν(CN), 1553 1455 ν(Ar–CC), 1323 ν(C–O), 561 ν(Zn–O), 430 ν(Zn–N); UV-Vis (λ_{max} nm^{-1}) (DMF): 247, 278, 440; molar conductance (DMF): 26.47 Ohm^{-1} cm^2 mol^{-1}; μ_{eff} (B.M): diamagnetic.

2.4. *Analytical methods*

Metal contents of the complexes were analyzed by EDTA titration [19] after decomposing the organic matter with a mixture of $HClO_4$, H_2SO_4, and HNO_3 (1 : 1.5 : 2.5). Elemental analyses were carried out on an Elementar Vario EL III, Carlo Erba 1108 elemental analyzer at the Sophisticated Analytical Instrument Facility (SAIF), Central Drug Research Institute, Lucknow. Molar conductance of 10^{-3} mol L^{-1} solutions of the complexes in DMF was measured at room temperature with a Deep Vision Model-601 digital direct reading deluxe conductivity meter. Magnetic susceptibility measurements were carried out by employing the Gouy method at room temperature on a powder sample of the complex; $CuSO_4 \cdot 5H_2O$ was used as calibrant. Infrared spectra (IR) (4000–400 cm^{-1} KBr discs) of the samples were recorded on an FT-IR Affinity-1 spectrophotometer (Shimadzu). Electronic absorbance spectra from 200 to 1100 nm were recorded on a UV-1601 spectrophotometer

(Shimadzu). Proton nuclear magnetic resonance spectra of HL and its zinc complexes (300 MHz) were recorded on a Bruker Avance DRX-300 FT-NMR spectrometer using DMSO-d_6 as solvent. Tetramethylsilane was used as internal standard. Chemical shifts are reported in δ scale. EPR spectra of complexes in solid state at 300 K and frozen DMSO at 77 K were recorded on a Varian E-112 spectrometer at X-band using TCNE as marker with 100 kHz modulation frequency and 9.1 GHz microwave frequency. Mass spectrometry experiments were performed on a JEOL-AccuTOF JMS-T100LC mass spectrometer equipped with a custom-made electrospray interface (ESI).

2.5. *DNA interaction study*

2.5.1. Electronic absorption titration. All experiments involving interaction of **1**–**4** with DNA were carried out in 5 mmol L^{-1} Tris-HCl buffer at pH 7.2, containing 50 mmol L^{-1} NaCl. The DNA concentration per nucleotide was determined by absorption spectroscopy using the molar absorption coefficient (6600 (mol L^{-1})$^{-1}$ cm^{-1}) at 260 nm [20].

Absorption titration experiment was performed by maintaining the complex concentration at 10 μmol L^{-1} and gradually increasing the concentration (20–100 μmol L^{-1}) of nucleic acid. The complexes were dissolved in mixed DMF and Tris-HCl buffer. The reference cuvette also included this mixed solvent. Absorption spectra of each complex solution were scanned from 200 to 500 nm and then equal amount of ct-DNA was added to complex solution and the reference cuvette. After each cuvette was incubated at room temperature for 10 min, absorption spectra were recorded for the same wavelength range. The changes in the metal complex concentration because of adding DNA solution to each cuvette were negligible at the end of each titration. For **1**–**4**, the intrinsic binding constant (K_b) was determined from spectral titration data using the following equation [21]:

$$[\mathrm{DNA}]/(\varepsilon_a - \varepsilon_f) = [\mathrm{DNA}]/(\varepsilon_b - \varepsilon_f) + 1/K_b(\varepsilon_b - \varepsilon_f),$$

where [DNA] is the concentration of DNA in base pairs, the apparent absorption coefficients ε_a, ε_f, and ε_b correspond to A_{obsd}/[complex], the extinction coefficient of the free complex, and the extinction coefficient of the complex when fully bound to DNA, respectively. K_b is the equilibrium binding constant in (mol L^{-1})$^{-1}$.

2.5.2. Cyclic voltammetric experiments. Cyclic voltammetry studies were performed on a CH instrument electrochemical analyzer in a 15 mL three-electrode electrolytic cell. The working electrode was glassy carbon, platinum wire electrode was used as the counter electrode and an Ag/AgCl electrode saturated with KCl was used as reference electrode. Cyclic voltammograms of the complexes were recorded in 1 : 2 DMF : buffer solution at $\nu = 0.1$ Vs^{-1}, where the buffer solution was the supporting electrolyte. Oxygen was removed by purging the solution with nitrogen which had been previously saturated with solvent vapors. All electrochemical measurements were performed at 27°C.

2.5.3. Viscosity measurements. Viscosity measurements were carried out using an Ubbelodhe viscometer maintained at 37°C in a thermostatic bath. DNA samples

approximately 200 base pairs in average length were prepared by sonicating in order to minimize complexities arising from DNA flexibility [22]. Flow time was measured with a digital stopwatch, and each sample was measured three times, and an average flow time was calculated. Data were presented as $(\eta/\eta_0)^{1/3}$ *versus* binding ratio (R = [complex]/[DNA]) [23], where η is the viscosity of DNA in the presence of complex and η_0 is the viscosity of DNA alone.

2.5.4. DNA cleavage experiments. The DNA cleavage activity of newly synthesized complex **1** was studied by agarose gel electrophoresis. Supercoiled plasmid pBR322 DNA (0.3 μg), dissolved in 5 mmol L^{-1} Tris-HCl/50 mmol L^{-1} NaCl buffer (pH 7.2), was treated with all the complexes. The mixtures were incubated at 37°C for 1 h and then mixed with the loading buffer (2 μL) containing 25% bromophenol blue, 0.25% xylene cyanol, and 30% glycerol. Each sample (5 μL) was loaded into 1% agarose gel containing 1.0 μg mL^{-1} EB. Electrophoresis was undertaken for 2 h at 50 V in Tris-acetate-EDTA (TAE) buffer (pH 8.0). The DNA cleavage with added reductant or oxidant was monitored as in the case of cleavage experiment without added reductant or oxidant using agarose gel electrophoresis. The reaction was also monitored upon addition of various radical inhibitors, such as sodium azide (NaN_3), DMSO, superoxide dismutase (SOD), hydrogen peroxide (H_2O_2), and 3-mercaptopropionic acid (MPA), glutathione (GSH), ascorbic acid (Asc). The samples were incubated for 2 h at 37°C. The gel was stained with EB for 5 min after electrophoresis and then photographed under UV light. All experiments were carried out in triplicate under the same conditions.

2.6. *Antimicrobial studies*

The disc diffusion method was used to evaluate antimicrobial activities of HL and **1**–**4** [24]. Antimicrobial activities were assayed on different microorganisms, *Staphylococcus aureus, Bacillus subtilis, Escherichia coli, Pseudomonas aeruginosa, Aspergillus niger, Rhizopus stolonifer, Candida albicans,* and *Rhizoctonia bataicola* by the disc diffusion method. A lawn of microorganism was prepared by pipetting and evenly spreading 100 μL of inoculum into nutrient agar set in Petri discs. Paper discs were impregnated with stock solution of the samples and dried under sterile conditions. Then the dried discs were laid on the previously inoculated agar surface. The plates were incubated at 37°C. After 24 h, the activities of the complexes were observed. The experiments were repeated three times and the results were expressed in average values. A 10 μL spore suspension (10^5–10^6 spore mL^{-1}) of each of the investigated organisms was added to a sterile agar medium just before solidification, then poured into sterile Petri discs (9 cm in diameter), and left to solidify. The bacteria were subcultured in agar medium. The Petri discs were incubated for 24 h at 37°C. Standard antibacterial drug (Ciprofloxacin) was also screened under similar conditions for comparison. The fungi were subcultured in potato dextrose agar medium. Standard antifungal drug (fluconazole) was used for comparison. The Petri discs were incubated for 48 h at 37°C.

To understand quantitatively the antimicrobial activities of compounds their minimum inhibitory concentrations (MIC) were evaluated by the microdilution broth method [25]. Sample solutions were added to broth for different concentrations. Samples measuring of each microbial suspension were added to the serial dilution of the

test substances. The inoculated test tubes were incubated at 37°C under aerobic conditions. The MIC was defined as the lowest antimicrobial concentration of the test samples. Solvent control test was performed to study the effect of 10% DMSO on the growth of microorganism and it did not inhibit growth. All tests were performed in duplicate and MICs were constant.

3. Results and discussion

Four mixed-ligand complexes [M(L)(phen/bpy)Cl] (where M is Cu(II) and Zn(II), phen is 1,10-phenanthroline, and bpy is 2,2′-bipyridine) have been prepared by reaction of metal salts and Schiff base with phen/bpy. They have been characterized by elemental analysis, IR, UV-Visible, ^{1}H NMR, ESI-MS, and EPR spectroscopic methods.

3.1. *Molar conductance measurements*

From molar conductance measurements, the complexes are non-electrolytic nature in 10^{-3} mol L^{-1}DMF solution, implying the presence of chloride in the coordination sphere of the complexes.

3.2. *Electronic absorption spectra and magnetic susceptibility*

The electronic absorption spectra of HL and **1**–**4** were recorded in DMF. The Schiff-base ligand has ring $\pi \rightarrow \pi^*$ bands at 243 and 273 nm and a band at 335 nm due to $n \rightarrow \pi^*$ transition associated with the azomethine linkage. These bands show a bathochromic shift due to coordination of azomethine [26]. The moderately intense broad bands for **3** and **4** at 437–440 nm are assigned to metal-to-ligand charge transfer (MLCT) transition. The Zn(II) complexes show no appreciable absorption above 450 nm in DMF solution, in accord with the d^{10} electronic configuration of Zn(II). At room temperature, the magnetic moments of the Zn(II) complexes are zero and they are diamagnetic.

The electronic absorption spectra of **1** and **2** show a broad band centered at 656 nm and 638 nm, respectively, corresponding to $^2E_g \rightarrow {}^2T_{2g}$ transition, consistent with octahedral geometry around Cu(II). Bands at 431 nm for **1** and 435 nm for **2** are assigned to MLCT transfer and the remaining bands at 252 nm, 279 nm for **1** and at 248 nm, 275 nm for **2** are due to $\pi \rightarrow \pi^*$ transitions of coordinated phen and bpy ligand, respectively. The magnetic moment of the complexes (1.78 B.M. for **1** and 1.76 B.M. for **2**) at room temperature indicates monomeric Cu(II) complexes.

3.3. *IR spectral studies*

IR spectra of the complexes are compared with the free ligand to determine the coordination sites involved in chelation. HL shows a strong band at 1612 cm^{-1}, characteristic of the azomethine. Coordination of the Schiff base to metal through nitrogen is expected to reduce electron density in the azomethine. The band due to

azomethine nitrogen ν(C=N) shows a modest decrease in frequency for the complexes appearing around 1585–1600 cm^{-1}, consistent with coordination of the azomethine nitrogen [27]. The amide stretch, ν(CONH) of 2-methylacetoacetanilide of HL at 1670 cm^{-1}, shifts to 1654–1658 cm^{-1} upon coordination, indicating coordination of metal ion *via* amide carbonyl oxygen. There is an upward shift in the stretching frequency of ν(C–O) in the complexes from 1265 cm^{-1} to 1317–1325 cm^{-1}, further supported by the disappearance of ν(O–H) at 3375 cm^{-1} for all the complexes, indicating deprotonation of phenolic proton. The band at 3238 cm^{-1} (ν(NH)) does not change for ligand and complexes. Ring stretching frequencies (ν(C=C) and ν(C=N)) at 1506, 1420 cm^{-1} for free phen and 1528, 1455 cm^{-1} for free bpy shift to higher frequencies upon complexation (1514, 1423 cm^{-1} for **1**, 1548, 1467 cm^{-1} for **2**, 1517, 1425 cm^{-1} for **3**, and 1545, 1462 cm^{-1} for **4**), indicating coordination of the heterocyclic nitrogen. Absorptions at 555–565 and 423–435 cm^{-1} are ascribed to the formation of M–O and M–N bonds, respectively [28], further supporting coordination of the azomethine nitrogen and phenolic oxygen.

3.4. *^{1}H NMR spectral studies*

^{1}H NMR spectra of HL and **3** and **4** were recorded in DMSO-d_6. All the protons were in their expected regions. Observed signals for HL at 10.54, 8.95, and 6.82–7.90 ppm are attributed to phenolic OH, amide NH, and aromatic protons, respectively. Methylene protons at 3.35 ppm and methyl protons at 2.04 ppm for aliphatic (C–CH_3) and 2.48 ppm for aromatic (C–CH_3) are practically unaffected by complexation. In **3** and **4**, disappearance of phenolic OH proton ($\delta = 10.54$ ppm) is consistent with deprotonation and coordinating with zinc. Aromatic protons of **3** and **4** are at 6.84–8.61 and 6.83–8.48 ppm, respectively, and the signal of the NH ($\delta = 8.95$ ppm) is slightly changed, confirming the suggested structures of the complexes. The conclusions drawn from these studies lend further support to the mode of bonding discussed in IR spectra.

3.5. *Mass spectra of Schiff base and 1 and 2*

The ESI mass spectra of HL and its polypyridyl complexes **1** and **2** were carried out. The mass spectrum of HL showed a molecular ion peak at $m/z = 282$ $[M]^+$ and 283 $(M + 1)$, which is equivalent to its molecular weight. Complexes **1** and **2** showed characteristic molecular ion and ^{37}Cl isotopic peaks at m/z 560$[M]^+$, 562$(M + 2)$ and 536$[M]^+$, 538$(M + 2)$, respectively. The mass spectra of Schiff-base ligand and its polypyridyl complexes **1** and **2** are in agreement with the proposed structure (scheme 1).

3.6. *EPR spectra of 1 and 2*

X-band EPR spectra of **1** and **2** have been recorded at room temperature and DMSO solution at 77 K using 100 kHz field modulation; *g*-factors are quoted relative to the standard marker TCNE ($g = 2.00277$). EPR spectral assignments of **1** and **2** (77 K) along with the spin Hamiltonian and orbital reduction parameters are summarized in tables 1 and 2.

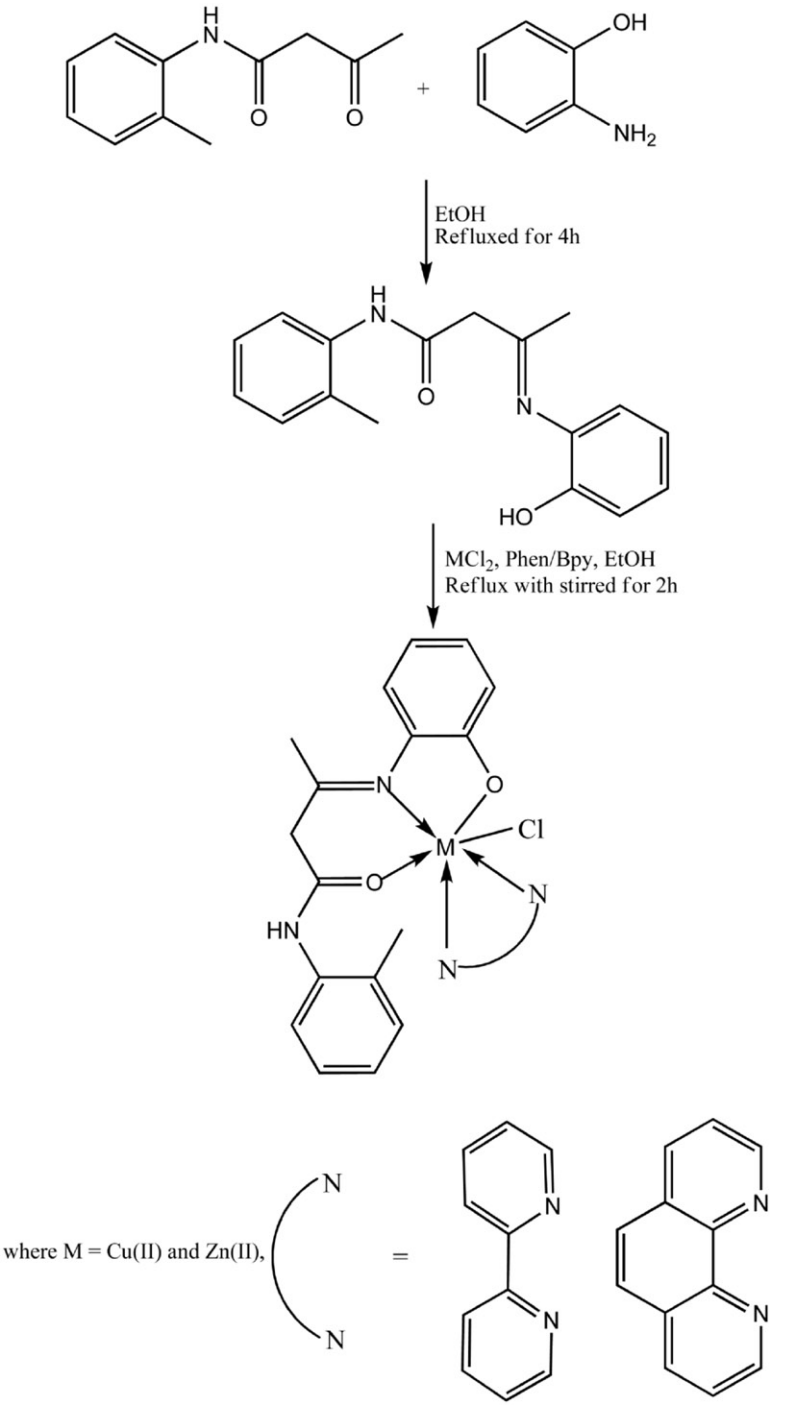

Scheme 1. Synthetic route of Schiff base and its complexes.

Table 1. The spin Hamiltonian parameters of **1** and **2** in DMSO at 77 K.

	g-tensor			Hyperfine constant $\times 10^{-4}$(cm^{-1})		
Complex	g	$g_\perp$	g_{av}	A	$A_\perp$	A_{av}
1	2.27	2.12	2.17	130	105	133.33
2	2.23	2.09	2.13	123	85	118.33

Table 2. The bonding parameters of **1** and **2** in DMSO at 77 K.

Complex	α^2	β^2	γ^2	K	$K_\perp$	K	G
1	0.72	0.88	0.95	0.61	0.74	0.32	2.279
2	0.65	0.82	0.93	0.52	0.63	0.29	2.60

EPR spectra of **1** and **2** in the polycrystalline state at 300 K show only one broad signal at $g_{iso} = 2.15$ and 2.12, respectively. Such isotropic spectra consisting of only one broad signal and hence only one g value which is due to polar broadening and enhanced spin lattice relaxation. Unfortunately, these spectra give no information on the electronic ground state of Cu(II) present in the complexes.

EPR spectra of **1** and **2** in DMSO at 77 K show well-resolved four hyperfine lines giving $g_{||} > g_\perp > 2.00277$, corresponding to the presence of an unpaired electron in the $d_{x^2-y^2}$ orbital. This reveals that the complexes are monomeric octahedral copper(II) species. The geometric parameter, $G = (g_{||} - 2.00277)/(g_\perp - 2.00277)$ values are less than 4.0, consistent with a copper(II) center in d_{x2-y2} ground state having small exchange coupling [29].

EPR parameters $g_{||}$, $g_\perp$, $A_{||}$, $A_\perp$ (Cu) and the energies of d–d transitions were used to evaluate bonding parameters α^2, β^2, and γ^2 which may be regarded as measures of the covalency of the in-plane σ-bonds, in-plane π-bonds, and out-of-plane π-bonds, respectively [30]. For a copper(II) complex, $g_{||}$ is sensitive to indicate covalence. The $g_{||}$ values for copper(II) complexes less than 2.3 indicate significant covalent bonding [31, 32].

In **1** and **2**, the value of in-plane σ-bonding parameter α^2 was estimated following Maki and McGarvey. These complexes have $K_{||} < K_\perp$, which suggests stronger in-plane π-bonding [33, 34]. The values of the bonding parameters α^2 (0.65–0.72), β^2 (0.82–0.88), and γ^2 (0.93–0.95) < 1.0 (value of 1.0 for 100% ionic character) indicate significant in-plane π-bonding and in-plane σ-bonding while the axial bond is more polar. The Fermi contact hyperfine interaction term $K = A_{iso}/P\beta^2 + (g_{av} - 2.00277)/\beta^2$ is a measure of the contribution of the 's' electrons to the hyperfine interaction, found to be 0.29–0.32. The calculated empirical factor $f = g_{||}/A_{||}$ values (175 cm for **1** and 181 cm for **2**) and index of tetragonal distortion are higher than the range 105–135 supporting high distortion from octahedral geometry.

3.7. *DNA-binding and cleavage properties*

DNA is the primary pharmacological target of many antitumor compounds [35] and interactions of metal complexes with DNA have been a subject of importance for

Table 3. Electronic absorption spectral properties of **1**–**4** with ct-DNA.

	λ_{max} (nm)				
Complex	Free	Bound	$\Delta\lambda$ (nm)	Hypochromicity (%)	$K_b \times 10^4$ $((mol\,L^{-1})^{-1})$
1	431.0	435.5	4.5	12.53	5.72
2	435.0	438.0	3.0	14.50	1.55
3	437.5	440.0	2.5	34.47	2.06
4	440.4	442.3	1.9	26.36	0.98

development of effective chemotherapeutic agents. For this reason, before investigating the nuclease activity of the compound, we carried out absorption titration, viscosity measurements, and cyclic voltammetry to examine the complexes mode of, and propensity for, binding to ct-DNA.

3.7.1. Absorption titration study of complex-DNA interaction. The binding ability of the complexes with ct-DNA can be characterized by measuring their effects on absorption spectra. Complex binding with DNA through intercalation usually result in hypochromism and bathochromism due to the strong stacking interaction between an aromatic chromophore and the base pairs of DNA [36]. In the present investigation, the interaction of the bpy- and phen-based complexes (**1**–**4**) in DMF solutions (10%) with ct-DNA have been investigated. Absorption titration experiments of the complexes in buffer were performed by using a fixed concentration of complexes to which increments of DNA stock solution were added. The binding of the complexes to duplex DNA led to a decrease in absorption intensities with a small red shift in the UV-Vis absorption spectra [37]. To compare quantitatively the affinity of the four complexes toward DNA, the binding constant (K_b) of the complexes to ct-DNA was determined by monitoring the changes of absorbance at 431 nm (for **1**), 435 nm (for **2**), 437.5 nm (for **3**), and 440.4 nm (for **4**) with increasing concentration of DNA. The binding constants (K_b) of complexes are 5.72×10^4, 1.55×10^4, 2.06×10^4, and 0.98×10^4 $(mol\,L^{-1})^{-1}$, respectively (table 3). These K_b values are lower than those observed for classical intercalators (e.g. EB-DNA, $\sim 10^6\,(mol\,L^{-1})^{-1}$) [38], but have the same level as those of some well-established intercalation agents ($\sim 10^4$) [39–42]. Better binding affinity of phen complexes to ct-DNA than bpy complexes may be due to the extended aromaticity and coplanarity of the phenanthroline ring system for better stacking between the base pairs of DNA [43]. These spectral characteristics suggest that all four complexes interact with DNA, likely through intercalation. The absorption titration of **1** is shown in figure 1.

3.7.2. Cyclic voltammetric study of complex-DNA interaction. Redox behaviors of **1**–**4** in the absence and presence of ct-DNA were studied in DMF : buffer (1 : 2) by cyclic voltammetry at room temperature from 1.0 to −1.2 V. Cyclic voltammetry is an important electroanalytical technique for studying interaction of metal complexes with biomolecules due to the similarity between various chemical and biological redox processes [44, 45].

Cyclic voltammograms (CV) of **1** and **2** exhibit two quasi-reversible redox waves corresponding to Cu(III)/Cu(II) and Cu(II)/Cu(I) couple with E_{pc} and E_{pa} values

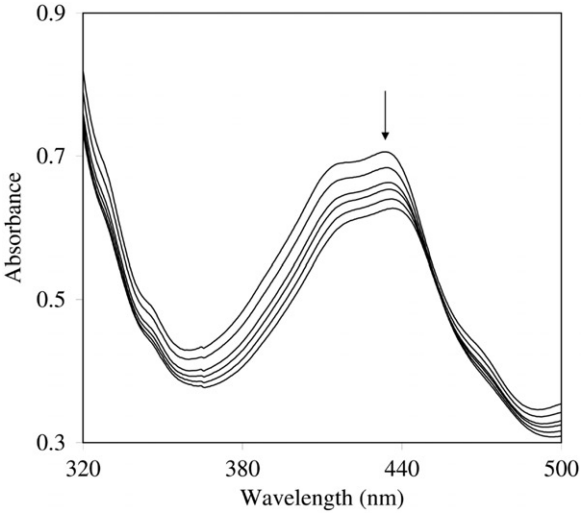

Figure 1. Absorption spectrum of **1** in Tris-HCl buffer upon addition of ct-DNA. [complex] = 10 μmol L^{-1}, [DNA] = (20–100) μmol L^{-1}. The arrow shows the absorbance changing upon increasing DNA concentration.

−0.048, −0.445 V and −0.069, −0.101 V for **1** and −0.122, −0.561 V and −0.105, −0.089 V for **2** at 0.1 V s^{-1} scan rate. The ratio of anodic to cathodic peak currents I_{pa}/I_{pc} was less than 1.0. The formal electrode potentials $E_{1/2}$ and ΔE_p for Cu(III)/Cu(II) and Cu(II)/Cu(I) couple (difference in cathodic E_{pc} and anodic E_{pa} peak potentials) were 0.010, −0.274 V and 0.117, 0.347 V for **1** and −0.017, −0.650 V and 0.227, 0.472 V for **2**. The ΔE_p values are larger than the Nernstian values observed for a one-electron transfer redox couple [46]. At constant parameters, the addition of ct-DNA shifts $E_{1/2}$, ΔE_p values for the above-mentioned two redox couples to 0.006, −0.243 V and 0.184, 0.306 V for **1** and −0.084, −0.632 V and 0.212, 0.242 V for **2** (figure 2). The ratios of I_{pa}/I_{pc} were also less than unity for ct-DNA bound complexes. The shift in potentials and decrease in current ratio suggest binding of **1** and **2** to ct-DNA [47].

The CV of **3** and **4** in DMF : buffer (1 : 2) solution at a scan rate 0.1 V s^{-1} features a quasi-reversible redox wave Zn(II)/Zn(I) with $E_{1/2}$(−0.510), ΔE_p(0.725) for **3** and $E_{1/2}$(−0.375), ΔE_p(0.378) for **4** [48]. Upon addition of ct-DNA under the same conditions, complexes experience a shift in $E_{1/2}$(−0.503), ΔE_p(0.656) for **3** and $E_{1/2}$(−0.362), ΔE_p(0.323) for **4** (table 4). The ratio of anodic to cathodic peak currents (I_{pa}/I_{pc}) in the presence and absence of DNA with zinc complexes was less than unity.

The shift in $E_{1/2}$ for complexes on binding to DNA suggests that both M(II) and M(I) forms bind but to different extents. Analogous to the treatment of the association of small molecules with micelles and DNA [49, 50], the ratio of the equilibrium constants, K_R/K_O for binding of the M(II) and M(I) forms of complexes to DNA can be estimated from the net shift in $E_{1/2}$. For a Nernstian electron transfer in a system in which both the oxidized and reduced forms associate with a third species such as DNA in solution can be applied. Here, M^{n+}-DNA represents metal complexes bound to DNA with $n+$ charge on the metal center. Thus for one-electron transfer,

$$E_b^\circ - E_f^\circ = 0.0591 \log(K_R/K_O),$$

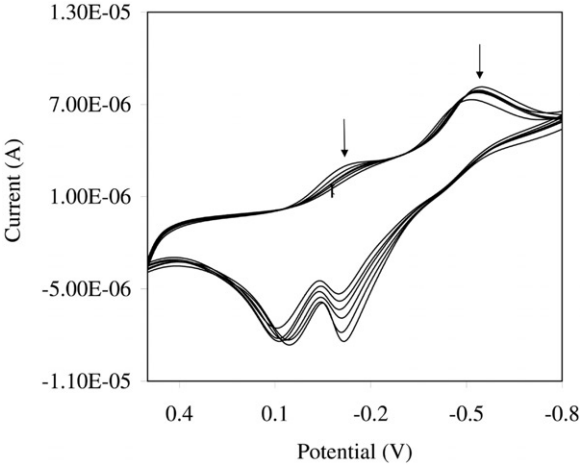

Figure 2. Cyclic voltammogram of **2** in the absence and presence of increasing amounts of ct-DNA at room temperature in DMF : Tris-HCl buffer (1 : 2) mixture (pH 7.2) (scan rate = 0.1 V s^{-1}). The arrow shows the current changing upon increasing DNA concentration.

Table 4. Electrochemical behavior of **1–4** in the absence and presence of ct-DNA.

		E_{pc} (V)		E_{pa} (V)		ΔE_p (V)		$E_{1/2}$ (V)		
Complex	Redox couple	Free	Bound	Free	Bound	Free	Bound	Free	Bound	K_R/K_O
1	Cu(III)/Cu(II)	−0.048	−0.089	0.069	0.095	0.117	0.184	0.010	0.006	0.20
	Cu(II)/Cu(I)	−0.448	−0.396	−0.101	−0.090	0.347	0.306	−0.274	−0.243	7.45
2	Cu(III)/Cu(II)	−0.122	−0.148	0.105	0.064	0.227	0.212	−0.017	−0.084	0.36
	Cu(II)/Cu(I)	−0.561	−0.528	−0.089	−0.104	0.474	0.424	−0.650	−0.632	3.61
3	Zn(II)/Zn(I)	−0.873	−0.831	−0.148	−0.175	0.725	0.656	−0.510	−0.503	5.06
4	Zn(II)/Zn(I)	−0.564	−0.524	−0.186	−0.201	0.378	0.323	−0.375	−0.362	4.33

where E_f° and E_b° are the formal potentials of the M(II)/M(I) couple in the free and fully bound forms, respectively. K_R and K_O are the corresponding binding constants for the M^{2+} and M^+ species to DNA. The binding ratios of the phen-complexes are higher than the bpy-complexes. These values suggest that the interaction of metal complexes with DNA tends to stabilize the M(II) over M(I) (table 4). Based on the above CV data, all the complexes bind to DNA by both intercalation and electrostatic interaction.

3.7.3. Viscosity measurements. Viscosity is a useful technique for exploring the binding mode of complexes with ct-DNA, considered as least ambiguous and most critical test of binding in solution. A classical intercalator causes a significant increase in the viscosity of DNA solution due to increase in overall DNA contour length [51]. A partial or non-classical intercalation of metal complexes reduces the DNA viscosity [52]. The effect of phen and bpy complexes on the viscosity of ct-DNA is

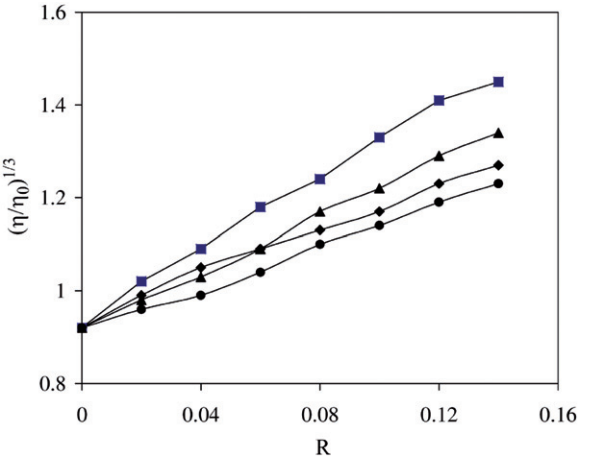

Figure 3. Change in relative specific viscosity of ct-DNA (10×10^{-5} mol L^{-1}) on addition of **1** (■), **2** (◆), **3** (▲), and **4** (●) in Tris-HCl buffer (pH 7.2) at 37°C, R = [complex]/[DNA].

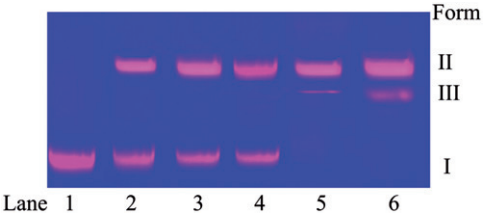

Figure 4. Agarose gel electrophoresis pattern showing cleavage of pBR322 DNA (0.3 μg) by **1**. Lane 1, DNA; Lane 2, DNA + **1** (20 μmol L^{-1}); Lane 3, DNA + **1** (40 μmol L^{-1}); Lane 4, DNA + **1** (60 μmol L^{-1}); Lane 5, DNA + **1** (80 μmol L^{-1}); Lane 6, DNA + **1** (100 μmol L^{-1}).

shown in figure 3. The plots show relative viscosity increases with increase in concentration of complexes. The observed order of DNA-binding in viscosity measurements is **1** > **3** > **2** > **4**, rationalized by intercalation.

3.7.4. DNA cleavage activity of 1. Since **1** shows highest binding tendency with ct-DNA, the cleavage activity has been evaluated for **1**. The nuclease activity of **1** has been studied using supercoiled pBR322 DNA as substrate. To discover the DNA cleavage ability, supercoiled pBR322 DNA was incubated with different concentrations of complex in aqueous buffer solution (5 mmol L^{-1} Tris-HCl/50 mmol L^{-1} NaCl, pH 7.2) without addition of any reductant or oxidant. The DNA-cleaving ability of **1** was demonstrated initially by a plasmid relaxation assay, in which conversion of supercoiled form (Form I, SC) to nicked circular (Form II, NC) or linear open circular (Form III, LC) DNA was monitored. As observed from figure 4, there is a gradual decrease in the amount of Form I with a simultaneous increase in Form II (Lanes 2 and 3) on increasing the concentration of the complex. A notable cleavage feature observed for **1** is the appearance of Form III before the disappearance of Form I (Lanes 3 and 4).

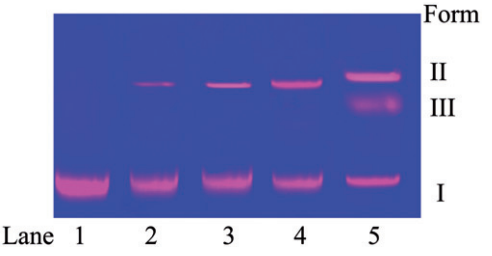

Figure 5. Agarose gel electrophoresis pattern for cleavage of pBR322 DNA (0.3 μg) by **1** (40 μmol L^{-1}) in the presence of different activating agents at 37°C after incubation for 2 h. Lane 1, DNA control; Lane 2, DNA + **1** + GSH (40 μmol L^{-1}); Lane 3, DNA + **1** + Asc (40 μmol L^{-1}); Lane 4, DNA + **1** + MPA (40 μmol L^{-1}); Lane 5, DNA + **1** + H_2O_2 (40 μmol L^{-1}).

This indicates that **1** is capable of direct strand scission and is better suited for therapeutic applications, while many complexes are only able to cleave a single strand successively [53].

The cleavage efficiency of copper(II) is usually dependent on activators. Therefore, to understand the cleavage mechanism, a lower concentration (40 μmol L^{-1}) of **1** was allowed to stay in the presence of activators, namely H_2O_2 and MPA, GSH, Asc; **1** showed significant increase in the cleavage of DNA in the order H_2O_2 > MPA > Asc > GSH (figure 5).

Experiments were carried out in the presence of several reactive oxygen trappers since dioxygen or redox reagents are believed to be a major cause of DNA damage. To investigate this mechanistic pathway of DNA cleavage, **1** (80 μmol L^{-1}) was allowed to interact with DNA separately with DMSO (Lane 2) and ethanol (Lane 3) as a hydroxyl radical scavenger under identical conditions; cleavage was not significant as compared to DNA cleavage without them. Therefore, it was considered that diffusible ($^{\bullet}OH$) hydroxyl radicals are not responsible for DNA cleavage. However, with other oxygen trappers like sodium azide (NaN_3) as singlet oxygen scavenger, the cleavage was significant, revealing the involvement of $^1O_2$ in DNA cleavage (Lane 4). The involvement of $^1O_2$ was further supported by significant enhancement of the cleavage activity in D_2O, where lifetime of $^1O_2$ is longer than in water [54]. In D_2O, a linear form also appeared, indicating increase in cleavage (Lane 5). In the presence of superoxide dismutase (SOD), a facile superoxide anion radical ($O_2^{\bullet-}$) quencher, cleavage was observed similar to that observed in the presence of complex only (Lane 6), revealing that superoxide anion is not the active species in cleavage of DNA as depicted in figure 6. Hence, the cleavage pattern supports the oxidative cleavage pathway.

3.8. *Antimicrobial effect*

In vitro testing of antibacterial and antifungal activities of the ligand and **1**–**4** are shown in table 5. For comparison, MIC values of ciprofloxacin and fluconazole are also listed in table 5. The ligand and complexes showed different degrees of antimicrobial activities. In antibacterial studies, **1** has good activity against *S. aureus* and *E. coli* (MIC = 3.125 μg mL^{-1}) compared to other complexes and also other tested microorganisms. Complexes **2**, **3**, and **4** have lowest antibacterial activity against *P. aeruginosa* (MIC = 25 μg mL^{-1}) and *B. subtilis* (MIC = 25–50 μg mL^{-1}), respectively. In antifungal

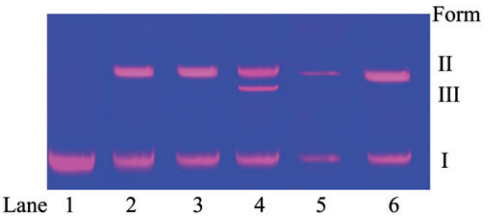

Figure 6. Agarose gel electrophoresis pattern showing cleavage of pBR322 DNA (0.3 μg) by **1** (80 μmol L^{-1}) in the presence of standard radical scavengers at 37°C after incubation for 2 h. Lane 1, DNA control; Lane 2, DNA + **1** + DMSO (15 Units); Lane 3, DNA + **1** + ethanol (15 Units); Lane 4, DNA + **1** + D_2O (70 %); Lane 5, DNA + **1** + NaN_3 (0.4 mmol L^{-1}); Lane 6, DNA + **1** + SOD (15 Units), respectively.

Table 5. The *in vitro* antimicrobial activity of HL and **1**–**4** evaluated by MIC.

	Antibacterial activity				Antifungal activity			
Complex	*S. aureus*	*B. subtilis*	*E. coli*	*P. aeruginosa*	*A. niger*	*R. bataicola*	*R. stolonifer*	*C. albicans*
HL	100	200	100	200	100	100	100	200
1	3.125	12.5	3.125	6.25	6.25	12.5	6.25	25
2	12.5	6.25	6.25	25	12.5	25	12.5	50
3	6.25	25	6.25	12.5	3.125	12.5	6.25	12.5
4	12.5	50	12.5	25	12.5	6.25	25	50
Ciprofloxacin	0.78	1.56	0.78	1.56	–	–	–	–
Fluconazole	–	–	–	–	0.78	1.56	1.56	1.56

studies, **3** has greatest activity against *A. niger* (MIC = 3.125 μg mL^{-1}), while **2** and **4** have moderate activity against *C. albicans* (MIC = 50 μg mL^{-1}). All compounds have low to moderate activity compared to ciprofloxacin and fluconazole. Comparison to the previously reported 2-methylacetoacetanilide Schiff base and copper and zinc complexes [55, 56], the present complexes are better, perhaps due to phen/bpy and chloride inside the coordination sphere. In general, the enhancement of metal complexes in the activity can be explained on the basis of Tweedy's chelation theory [57].

4. Conclusion

Synthesis and spectral characterization of Schiff-base polypyridyl copper and zinc complexes are reported in this work. The Schiff base is tridentate and phen/bpy are bidentate. Complexes **1**–**4** adopt octahedral geometry around the metal. DNA-binding studies reveal that **1** has more intercalative binding than **2**–**4**. Complex **1** shows significant increase in cleavage of pBR322 DNA and the order of cleavage in different activators is H_2O_2 > MPA > Asc > GSH. Complex **1** cleaves pBR322 DNA effectively *via* oxidative pathway. The antimicrobial activities reveal that ligand and complexes have antimicrobial activity, depending on the microbial species tested. None of the present compounds are as effective against the tested microorganisms as currently used drugs.

Acknowledgments

The authors express their heartfelt thanks to the College Managing Board, Principal, and Head of the Department of Chemistry, VHNSN College, for providing necessary research facilities. SAIF, IIT Bombay and CDRI, Lucknow, are gratefully acknowledged for providing instrumental facilities.

References

[1] B. Chesneau, A. Passelande, P. Hudhomme. *Org. Lett.*, **11**, 649 (2009).
[2] G. Accorsi, A. Listorti, K. Yoosaf, N. Armaroli. *Chem. Soc. Rev.*, **38**, 1690 (2009).
[3] S. Anbu, M. Kandaswamy. *Polyhedron*, **30**, 123 (2011).
[4] L.F. Chin, S.M. Kong, H.L. Seng, K.S. Khoo, R Vikneswaran, S.G. Teoh, M. Ahmad, S.B.A. Khoo, M.J. Maah, C.H. Ng. *J. Inorg. Biochem.*, **105**, 221 (2011).
[5] A. Yazici, F. Akgun. *Trans. Met. Chem.*, **31**, 152 (2006).
[6] P.U. Maheswari, M. Palaniandavar. *J. Inorg. Biochem.*, **98**, 219 (2004).
[7] K.E. Erkkila, D.T. Odom, J.K. Barton. *Chem. Rev.*, **99**, 2777 (1999).
[8] L.-N. Ji, X.-H. Zou, J.-G. Liu. *Coord. Chem. Rev.*, **216**, 513 (2001).
[9] S.O. Kelly, J.K. Barton, A. Sigel, H. Sigel. *Metal Ions in Biological Systems*, Marcel Dekker, New York (1998).
[10] H.H. Thorp. *Adv. Inorg. Chem.*, **43**, 127 (1995).
[11] P. De Hoog, M.J. Louwerse, P. Gamez, M. Pitie, E.J. Baerends, B. Meunier, J. Reedijk. *Eur. J. Inorg. Chem.*, 612 (2008).
[12] S. Kumar, D.N. Dhar, P.N. Saxena. *J. Sci. Ind. Res.*, **68**, 181 (2009).
[13] A. Diaz, R. Villalonga, R. Cao. *J. Coord. Chem.*, **62**, 100 (2009).
[14] J.W. Choi, S.K. Kim. *Ann. Clin. Lab. Sci.*, **35**, 428 (2005).
[15] B.P. Goodman, E.P. Bosch, M.A. Ross. *J. Neurol. Neurosurg. Psychiatry*, **80**, 524 (2009).
[16] C Marzano, M. Pellei, F. Tisato. *Anti-Cancer Agents Med. Chem.*, **9**, 185 (2009).
[17] B. Coyle, K. Kavanagh, M. McCann. *Biometals*, **16**, 321 (2003).
[18] N. Raman, A. Selvan. *J. Mol. Struct.*, **985**, 173 (2011).
[19] A.I. Vogel. *Textbook of Quantitative Inorganic Analysis*, 4th Edn, ELBS and Longman, London (1978).
[20] M.F. Reichmann, S.A. Rice, C.A. Thomas, P. Doty. *J. Am. Chem. Soc.*, **76**, 3047 (1954).
[21] A. Wolfe, G.H. Shimer, T. Meehan. *Biochemistry*, **26**, 6392 (1987).
[22] J.B. Chaires, N. Dattagupta, D.M. Crothers. *Biochemistry*, **21**, 3933 (1982).
[23] G. Cohen, H. Eisenberg. *Biopolymers*, **8**, 45 (1969).
[24] R. Senthil Kumar, S. Arunachalam. *Eur. J. Med. Chem.*, **44**, 1878 (2009).
[25] M.C. Rodrıguez-Arguelles, E.C. Lopez-Silva, J. Sanmartın, P. Pelagatti, F. Zani. *J. Inorg. Biochem.*, **99**, 2231 (2005).
[26] A.D. Naik, V.K. Revankar. *Proc. Indian Acad. Sci. (Chem. Sci.)*, **113**, 285 (2001).
[27] K. Serbest, H. Kayi, M. Er, K. Sancak, I. Degirmencioglu. *Heteroatom Chem.*, **19**, 700 (2008).
[28] B.S. Creaven, M. Devereux, A. Foltyn, S. McClean, G. Rosair, V.R. Thangella, M. Walsh. *Polyhedron*, **29**, 813 (2010).
[29] M.J. Bew, B.J. Hathaway, R.R. Faraday. *J. Chem. Soc., Dalton Trans.*, 1229 (1972).
[30] A.H. Maki, B.R. McGarvey. *J. Chem. Phys.*, **29**, 31 (1958).
[31] A.H. Maki, B.R. McGarvey. *J. Chem. Phys.*, **29**, 35 (1958).
[32] J.R. Wasson, C. Trapp. *J. Phys. Chem.*, **73**, 3763 (1969).
[33] D. Kivelson, R. Neiman. *J. Chem. Phys.*, **35**, 149 (1961).
[34] B.J. Hathaway, G. Wilkinson, R.D. Gillard, J.A. McCleverty. *Comprehensive Coordination Chemistry*, Vol. 5, Pergamon Press, Oxford (1987).
[35] K.J. Du, J.Q. Wang, J.F. Kou, G.Y. Li, L.L. Wang, H. Chao, L.N. Ji. *Eur. J. Med. Chem.*, **105**, 1056 (2011).
[36] B. Peng, H. Chao, B. Sun, H. Li, F. Gao, L.N. Ji. *J. Inorg. Biochem.*, **100**, 1487 (2006).
[37] V. Uma, M. Kanthimathi, T. Weyhermuller, B. Unni Nair. *J. Inorg. Biochem.*, **99**, 2299 (2005).
[38] M. Baldini, M. Belicchi-Ferrari, F. Bisceglie, P.P. Dall' Aglio, G. Pelosi, S. Pinelli, P. Tarasconi. *Inorg. Chem.*, **43**, 7170 (2004).
[39] E.J. Gao, L. Wang, M.-C. Zhu, L. Liu, W.Z. Zhang. *Eur. J. Med. Chem.*, **45**, 311 (2010).
[40] N. Raman, K. Pothiraj, T. Baskaran. *J. Coord. Chem.*, **64**, 3900 (2011).
[41] M. Shakira, S. Khanam, M. Azam, M. Aatif, F. Firdaus. *J. Coord. Chem.*, **64**, 3158 (2011).

[42] N. Raman, K. Pothiraj, T. Baskaran. *J. Coord. Chem.*, **64**, 4286 (2011).
[43] P.K. Sasmal, A.K. Patra, M. Nethaji, A.R. Chakravarty. *Inorg. Chem.*, **45**, 11112 (2007).
[44] H.C. Hodges, M.A. Araujo. *Inorg. Chem.*, **21**, 3236 (1982).
[45] C.W. Lee, F.C. Anson. *Inorg. Chem.*, **23**, 837 (1984).
[46] N. Zhang, X. Zhang, Y. Zhao. *Talanta*, **62**, 1041 (2004).
[47] A.J. Bard, L.R. Faulkner. *Electrochemical Methods*, Wiley, New York (1980).
[48] X. Lu, K. Zhu, M. Zhang, H. Liu, J. Kang. *J. Biochem. Biophys. Methods*, **52**, 189 (2002).
[49] M.T. Carter, M. Rodriguez, A.J. Bard. *J. Am. Chem. Soc.*, **111**, 8901 (1989).
[50] L.S. Lerman. *J. Mol. Biol.*, **3**, 18 (1961).
[51] J. Liu, T.B. Lu, H. Deng, L.N. Ji. *Trans. Met. Chem.*, **28**, 116 (2003).
[52] Y.X. Xiong, F. He, X.H. Zou, J.Z. Wu, X.M. Chen, L.N. Ji, R.H. Li, J.Y. Zhou, K.B. Yu. *J. Chem. Soc., Dalton Trans.*, 19 (1999).
[53] Y. Jung, S.J. Lippard. *Chem. Rev.*, **107**, 1387 (2007).
[54] D. Lahiri, T. Bhowmick, B. Pathak, O. Shameema, A.K. Patra, S. Ramakumar, A.R. Chakravarty. *Inorg. Chem.*, **48**, 339 (2009).
[55] N. Raman, K. Pothiraj, T. Baskaran. *J. Mol. Struct.*, **1000**, 135 (2011).
[56] M. Manjunatha, V.H. Naik, A.D. Kulkarni, S.A. Patil. *J. Coord. Chem.*, **64**, 4264 (2011).
[57] B.G. Tweedy. *Phytopathology*, **55**, 910 (1964).